Assessing the degradation of compliant electrodes for soft actuators

by S. Rosset, C. de Saint-Aubin, A. Poulin, and H. Shea
EPFL, Switzerlnad

Review of Scientific Instruments, 88, 105002 (2017)

doi: 10.1063/1.4989464

Assessing the degradation of compliant electrodes for soft actuators

Samuel Rosset,[1, a)] Christine de Saint-Aubin,[1] Alexandre Poulin,[1] and Herbert R. Shea[1]
École polytechnique fédérale de Lausanne (EPFL), Neuchâtel, Switzerland

We present an automated system to measure the degradation of compliant electrodes used in dielectric elastomer actuators (DEAs) over millions of cycles. Electrodes for DEAs generally experience biaxial linear strains of more than 10 %. The decrease in electrode conductivity induced by this repeated fast mechanical deformation impacts the bandwidth of the actuator and its strain homogeneity. Changes in the electrode mechanical properties lead to reduced actuation strain. Rather than using an external actuator to periodically deform the electrodes, our measurement method consists of measuring the properties of an electrode in an expanding circle DEA. A programmable high voltage power supply drives the actuator with a square signal up to 1 kHz, periodically actuating the DEA, and thus stretching the electrodes. The DEA strain is monitored with a USB camera while the resistance of the ground electrode is measured with a multimeter. The system can be used for any type of electrode. We validated the test setup by characterising a carbon black/silicone composite that we commonly use as compliant electrode. Although the composite is well-suited for tens of millions of cycles of actuation below 5 %, we observe important degradation for higher deformations. When activated at 20 % radial strain, the electrodes suffer from important damage after a few thousand cycles, and an inhomogeneous actuation is observed, with the strain localised in a sub-region of the actuator only.

Keywords: dielectric elastomer actuators; compliant electrodes; degradation; lifetime

I. INTRODUCTION

Dielectric elastomers actuators (DEAs) consist of a thin (10 µm to 50 µm) and soft (Young modulus of about 1 MPa) elastomer membrane sandwiched between two compliant electrodes[1]. Compared to mainstream actuation technologies based on rigid materials, such as piezoelectric-actuators, or thermal and electrostatic microelectromechanical systems, DEAs are capable of very large actuation strains over 100%[2]. While most of the earlier literature on the subject concentrated on reaching the largest possible strain (1700% surface strain has been demonstrated[3]) without much consideration on lifetime and reliability, the maturation of the field, and the interest of industry for applications based on the technology, has pushed the research community to develop actuators that can survive for more than a few cycles. Consequently, it has become necessary to study and optimise the lifetime of dielectric elastomer actuators in order to meet the requirements of industrial applications.

Here, we present an automated measurement setup to characterise the ageing of the compliant electrodes of DEAs when cyclically actuated. The *novel electrode resistance degradation* (NERD) setup consists of an in-plane expanding circle actuator[2,4] connected to a programmable high voltage power-supply and to a four-wire resistance measurement system. A camera and image analysis routines enable the measurement of the actuation strain. The actuator is driven with a square signal, and the resistance and actuation strain are measured both in the activated and inactivated states. The evolution of these values can be analysed over a large number of cycles. Different electrode materials and application/patterning methods can be quickly tested, compared, and optimised to improve the lifetime of DEAs.

Due to their large strain and compliant nature, DEAs enable unprecedented performance in a large array of applications, including soft robotic manipulators, haptic feedback, tunable optics, biomedical applications, or microfluidics[5,6]. The DEA structure (soft membrane sandwiched between compliant electrodes) can also be deformed by an external force and serve as a soft stretch sensor or as an energy harvesting device[5,6]. One common point between all these applications is the large number of cycles the transducers are required to survive in their lifetime. For example, a stacked energy harvester mounted in a shoe heel[7] should have a life time of about 1000 km, i.e. in the order of 1 million steps or cycles.

The role of the electrodes of DEAs is to distribute the charges over the surface that is activated, leading to the generation of a Maxwell pressure, and ultimately to the deformation of the structure. Because the electrodes are attached to the surface of the elastomer membrane, they are submitted to the same deformation as the dielectric layer, which can expand by more than 100 % in area[2]. Additionally, many applications involve periodic actuation, thus placing the electrodes in a higly demanding situation. Electrodes for DEAs are most of time hand-applied and made from carbon grease or loose carbon powder[8]. However, commercial applications require robust electrodes with a method to accurately and repeatedly pattern them with high resolution on the dielectric membrane. The electrode material and the patterning method define the properties of the electrodes, such as its initial resistance, the change of resistance when stretched, the stiffening impact of the electrodes on the dielectric membrane, and the degradation of the resistance when cyclically stretched. While the first three points are often investigated in detail, the lifetime and degradation of the electrodes remain largely unexplored.

[a)] Electronic mail: samuel.rosset@a3.epfl.ch

The few studies that have been performed on the lifetime and degradation of dielectric elastomer transducers have mainly concentrated on the degradation of the dielectric membrane, looking at properties such as fatigue, breakdown strength, Young modulus or permittivity[9–11]. Automated setups for the material characterisation of DEAs over large number of cycles have been reported in the literature[11,12]. In addition, electrodes with special properties to increase their lifetime have been proposed, such as self-clearing electrodes[13,14], but no systematic study of the degradation of different types of electrodes when cyclically stretched has been performed.

Electrically, and in a simplified lumped model, DEAs are a series RC circuit and the resistance of the electrodes determine the speed at which the charges can be brought to (and removed from) the surface of the dielectric. Most DEAs produced in research laboratories are made with an acrylic elastomer (VHB from 3M), which is highly visco-elastic and has an extremely low mechanical cut-off frequency. Thus, the electrical resistance of the electrodes is of secondary importance compared to other properties, such as their ability to stretch[15] or their mechanical impact on the actuator stiffness[16]. Indeed, even with extremely resistive electrodes, DEAs often remain mechanically – rather than electrically – limited. However, despite being stiffer and generating less actuation strain, silicone elastomers are being increasingly used as dielectric layer, due to their long lifetime and reduced mechanical losses, which enable high speed applications such as tuneable lenses[17] or industrial pneumatic valves[18]. Furthermore, DEAs typically require a driving electric field in the order of $100\,\mathrm{V\,\mu m^{-1}}$. To reduce the driving voltage of these devices (which usually lies around 5 kV), one solution consists in reducing the thickness of the dielectric[16,19], thus increasing the capacitance of the device. The use of silicone membranes for fast applications, and/or the usage of thin membranes to decrease the actuation voltage therefore both require electrodes that have a low initial resistivity, and whose resistance doesn't increase when cyclically stretched. Stretchable electrodes for DEAs are submitted to an intense mechanical stress during their lifetime, and it is important that the electrical bandwidth of the actuator does not reduce.

II. MEASURING THE DEGRADATION OF ELECTRODES

The standards for dielectric elastomer transducers[20] provide guidelines on how the resistance of compliant electrodes should be measured. To measure only the resistance of the electrodes and not the contact resistance, the standards recommend the use of a four-wire measurement approach. In addition, it is recommended to use a long and thin conductive strip and to calculate the surface (sheet) resistance of the electrode. Compliant electrodes are meant to be stretched, and hence measuring the resistance in a deformed state is necessary, as indicated in the document, but without giving much information on how it should be done.

When the lifetime of the dielectric membrane is evaluated, it is usually submitted to a quasi-static high electric field until breakdown is observed[10] to create a worst-case situation. However, to assess the lifetime and to study the degradation of electrodes, it is necessary to submit them to cyclic stretching. Therefore, it requires test setups which can mechanically deform and relax a compliant electrode in a way that is similar to the load case of a DEA, and which are capable to do so rapidly in order to accumulate stretching cycles in a reasonable amount of time.

In the next sections, we present two different approaches to study the degradation of electrodes that we have implemented in the past, highlighting their limitations. We then introduce a new measurement methodology for fast and efficient testing of the resistance of stretchable electrodes for DEAs, and their degradation, the novel electrode resistance degradation (NERD) setup.

A. Uniaxial extension

The easiest method of measuring the resistance of a compliant electrode under stretch is to mount the system proposed in the standards paper (c.f. section II) on a motorised stage (figure 1 A). This is the method we used to characterise the resistance of gold-implanted compliant electrodes[21] and inkjet-printed carbon electrodes[22].

Although easy to implement, this method has an important drawback: it submits the electrode to uniaxial strain. Indeed the electrode is stretched in the direction of traction, but it is compressed in the perpendicular direction. This is not equivalent to what happens in the case of a DEA, for which the strain is usually equi-biaxial. In equi-biaxial extension, the electrode is elongated in the two perpendicular directions, which is a much tougher mechanical stress for the compliant electrodes. It is expected that an electrode will degrade faster under equi-biaxial stretching compared to the uniaxial case obtained when stretching a long and narrow strip. Consequently, cyclically stretching a conductive strip is not representative to the mechanical stress to which the compliant electrodes of a DEA is submitted.

B. Van der Pauw structure

Ideally, the resistance of a compliant electrode for DEA should be measured under equi-biaxial extension, to mimic the strain of most DEAs. However, this is not a trivial task. A flat membrane inflated with an air pressure p deforms into a bubble whose apex is in a state of equi-biaxial extension. We have used this property previously to measure the hyperelastic mechanical properties of thin silicone membranes under equi-biaxial loading[23].

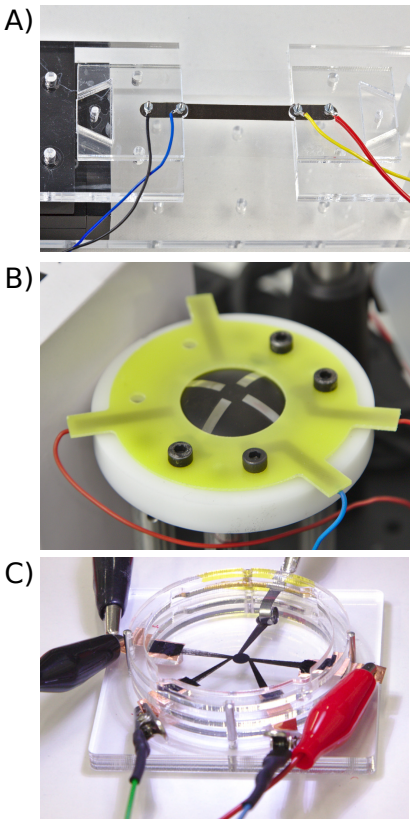

FIG. 1. Different methods to characterise the resistance of compliant electrodes under stretch and its dependance on cycle number. A) Uniaxial stretching of a compliant electrode by a motorised stage and 4-wire resistance measurement[22]. B) Equi-biaxial measurement of a van der Pauw structure printed on a membrane which is periodically inflated/deflated. C) NERD setup consisting of a 4-wire resistance measurement and strain tracking on an expanding circle dielectric elastomer actuator.

We used a similar approach to characterise the resistance of compliant electrodes. We printed a clover leaf pattern on a thin silicone membrane, which we inflated with a regulated pressure source to generate an equi-biaxial stretch (figure 1 B). A van der Pauw method[24,25] was used to measure the sheet resistance of the square at the centre of the membrane, and a camera looking horizontally at the membrane was used to extract the effective stretch of the probed area.

Although this approach enables to deform the compliant electrode under test equi-biaxially, it has one important drawback: the regulated pressure source and the closed loop control of the stretch via the camera lead to a quite slow inflation/deflation cycle of about 2 s. Consequently, characterising the evolution of the resistance over millions of cycles using a membrane inflated by an air pressure is too time consuming.

C. NERD

To address the important limitations of the two previous methods, we propose here a new test setup which consists in measuring the resistance of a circular actuator patterned on a prestretched membrane while it is being actuated at high voltage (figure 1 C).

When a dielectric with a low viscoelasticity (such as silicone) is used, the actuation – and therefore the ageing of the electrodes – can be performed quickly, typically at a few tens of Hertz. Thus, millions of actuation cycles can be achieved within a few hours. In addition, the electrodes are stretched equi-biaxially, which represents the harshest mechanical loading condition. Additional data can also be acquired, such as the actuation stretch as a function of applied voltage, which enables the evaluation of the stiffening impact of the electrodes. Because a high electric field is applied to stretch the electrodes, this measuring approach also makes it possible to evaluate the lifetime of the dielectric membrane.

In the next sections, we describe the measuring setup in detail and use it to characterise the ageing of compliant electrodes composed of carbon black dispersed into a silicone matrix, and patterned on the actuator by pad printing.

III. DESCRIPTION OF THE NERD MEASUREMENT SETUP

A. Measurement concept and actuator design

Among the many different possible actuator configurations, the in-plane expanding circle is often used as a benchmark to study the performance of DEAs[2,4,20,26]. It consists of an elastomer membrane prestretched equi-biaxially and fixed on a circular frame. At the centre of the membrane, circular compliant electrodes are patterned on both sides. When a voltage is applied to the electrodes, the generated Maxwell stress causes an increase of the diameter of the electrodes, which are therefore submitted to equi-biaxial extension.

The actuator used in the NERD setup is therefore an expanding circle actuator (figure 2 A). Unlike the usual expanding circle actuator for which each electrode has a single feed line from the edge of the membrane to the central active area[2,20], the NERD top electrode has 4 feed lines. Two of them (R_2), shown vertically on the figure, are used to inject a small measuring current, while the two others (R_1) are used to measure the voltage at the periphery of the circular active zone (R_a). The bottom electrode, on the backside of the membrane, has a single feed line (R_3), and the only overlapping region between the top and bottom electrodes is the central circular area (i.e. active area), which expands bi-axially when a voltage is applied as shown schematically on the cross-section of figure 2 B. A multimeter capable of doing 4-wire resistance measurements (Agilent 34410A, Keysight Tech-

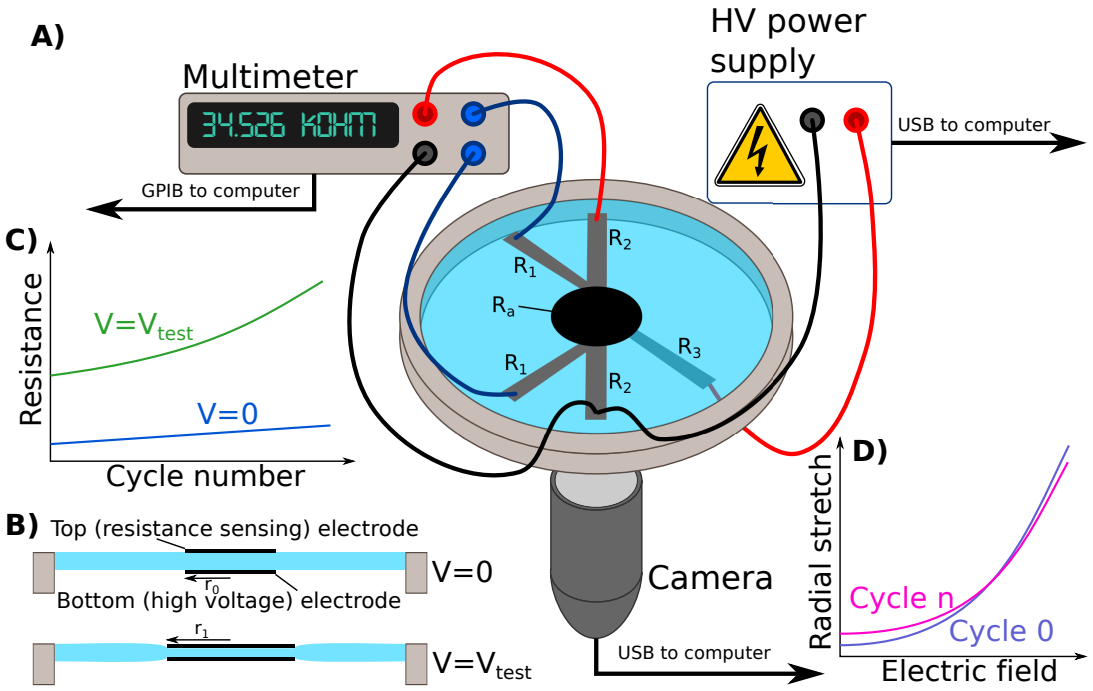

FIG. 2. A) NERD measurement setup. A circular DEA is manufactured on a prestretched silicone membrane. The active part (i.e. the part that stretches) is the central black circular area, which expands in diameter when a voltage is applied with a USB-controlled high voltage power supply. The actuation stretch is measured using a USB camera. The top electrode possesses 4 feed lines that enable 4-wire resistance measurement of the active zone of the electrodes with a multimeter connected to a computer. The voltage sensing lines (of resistance R_1) are positioned to measure only the resistance of the active zone, R_a. B) Schematic cross section of the actuator composed of the stretched dielectric membrane and 2 compliant electrodes. Upon application of a voltage, the radius of the electrode expands. C) The setup enables the measurement of the resistance of the active zone at rest and when activated, and to follow its evolution with the number of cycles. D) The setup enables the measurement of the stretch $\lambda = r_1/r_0$ as a function of the applied voltage, and to follow its evolution with the number of cycles.

nologies, or Keithley 2000, Keithley Instruments) is connected to the four terminals of the top electrode, and a programmable high voltage power supply (Peta-pico-Voltron[27]) is connected to the ground terminal of the top electrode and to the bottom electrode. Finally, a usb microscope (Dino-Lite Pro AM4113T5, AnMo Electronics Corporation) is mounted perpendicular to the membrane plane and is used to measure the expansion of the actuator when the high voltage is applied. The three instruments are connected to a computer running a LabVIEW programme controlling the measurement. The user chooses a stretch $\lambda = r_1/r_0$ at which the actuator should be cyclically actuated, where r_0 is the radius of the actuator at rest, and r_1 the radius of the activated device. The programme then computes the voltage V_{test} which must be applied in order to obtain the desired initial stretch λ, and cyclically activates the device at this voltage. It then analyses the evolution of the resistance at rest and when activated as a function of the number of cycles (figure 2 C), the evolution of the stretch as a function of cycles, the radial stretch as a function of electric field at different cycle numbers (figure 2 D), and the resistance as a function of stretch at different cycle numbers.

The measurement process is described in figure 3 and

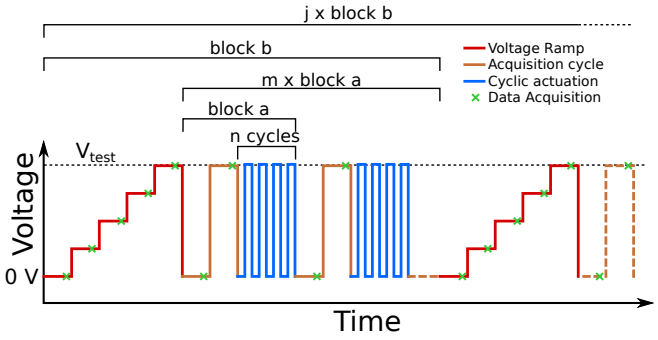

FIG. 3. The measurement process consists of two nested loops. The inner loop (block a) consists of a measurement phase during which the strain and electrode resistance are measured at rest and with the applied voltage V_{test}, followed by n cycles at high frequency to age the device without acquiring data. The outer loop (block b) consists in a voltage ramp from 0 to the set voltage to characterise the strain versus voltage and resistance versus voltage, followed by m blocks a. This block is repeated j times to make the complete test.

consists of two nested loops. The actuator stretch and resistance are measured at 0 V and at the voltage V_{test} (acquisition cycle). Each time data is acquired (green

x mark on the figure), the voltage is held at a constant value to give time for the actuator (strain and resistance) to stabilise. This holding time is usually of 5 s. The acquisition cycle is followed by rapid switching between 0 V and V_{test} for n cycles (usually several thousand) without recording data (cyclic actuation). The acquisition cycle and the cyclic actuation form block a, which is repeated m times. The number of switching cycles n within block a determine how often data is acquired (block a contains in fact $n+1$ cycle if one counts the acquisition cycle, but as n is usually large, the extra cycle can be neglected). The outer loop of the programme consists first of a voltage ramp from 0 to V_{test} with a number of steps specified by the user. The actuation stretch and electrode resistance are measured at each step, which allows to characterise the stretch versus voltage (or electric field), and the resistance versus stretch. The ramp is followed by m blocks a. This means that the stretch and resistance at rest and at maximum voltage are measured every n cycles, whereas the full ramp, which takes more time to perform, is measured far less often, every $m \times n$ cycles. Finally, the whole block b is repeated j times until the desired number of cycles for the measurement is achieved. Typically, blocks of 2000 cycles ($n = 2000$) are performed at 50 Hz, and repeated 25 times to have full ramps every 50'000 cycles ($m = 25$). Finally block b is repeated 20 times ($j = 20$) to reach 1 million cycles during the test.

The actuator diameter is 4 mm, located at the centre of a membrane with a diameter of 43 mm. This leads to a membrane to actuator diameter ratio larger than 10. The actuator must be much smaller than the membrane in order to maximise the size of the passive membrane which holds the prestretch, or else the actuation stretch will be reduced[4,28]. Koh et al. have shown that a ratio of membrane to actuator size larger than 10 should be used to minimise the effect of the finite membrane diameter. In addition, having a large membrane to actuator size ratio means that when the actuator expands upon activation, the contraction of the feed lines located on the passive membrane can be neglected. For a size ratio equal to 10, a radial stretch of λ of the electrode, leads to a stretch in the passive zone that can be estimated to $(10 - \lambda)/9$, although in reality it is position-dependent[4]. This means that upon activation of the actuator, only the part of the electrode located in the active area is stretched and sees its resistance change – as well as degrade – with the number of cycles. The resistance of the feed lines remains largely unaffected by the actuation.

B. Calculating the sheet resistance

The resistance measured by the multimeter enables to follow the degradation (or absence thereof) of the sample when cyclically activated by the high voltage power supply, and also to compare the initial resistance (and degradation) between different samples prepared to be used on the test setup. However, the absolute resistance

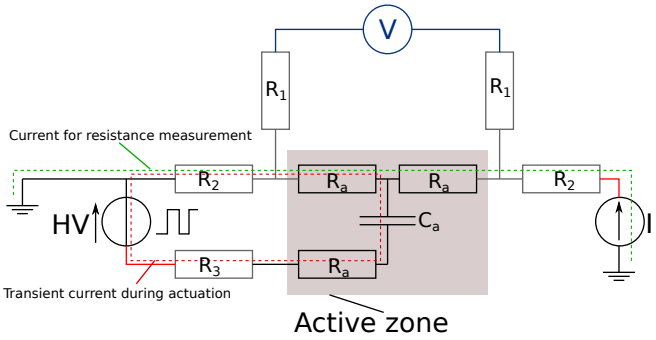

FIG. 4. Schematic electrical circuit of the test actuator. The multimeter in 4-wire resistance measurement mode can be separated into a current source I which injects a measurement current through the current feed lines R_2 (resistance names are the same as in fig. 2) and the circular electrode R_a, and a voltmeter V which probes the voltage through the feed lines R_1. A high voltage source HV is used to charge the capacitance of the active area C_a through the the active area resistance R_a and feed lines R_2 and R_3. Although represented here as lumped elements, the resistance of the active area R_a and its capacitance C_a form a 2D distributed RC network over the whole surface of the circular area.

in Ohms doesn't allow comparison with samples of different geometries, for example published by other research groups using rectangular electrodes. The sheet resistance (or, if the thickness of the electrode is known, the resistivity) of the electrode is a geometry-independent figure that makes it possible to compare samples. Obtaining the sheet resistance of a conductive material consists in dividing its resistance by the number of squares that form the resistive track. If this is easily done on long and thin test samples (hence the geometry recommended in the standards article[20], c.f. section II), the geometry of the actuator makes it more complicated. The NERD actuator is circular, and in addition, the current density is not homogeneous, as current is injected (and collected) at a small zone where the feed lines R_2 meet the circular region. This makes it difficult to analytically calculate the number of squares of the circular electrode of the actuator.

To measure the resistance of the expanding zone of the top electrode only, we use a 4-wire resistance measurement approach (figure 4). The multimeter sends a measuring current (green dashed line) through the circular electrode via the two feed lines R_2. The voltage is read by the multimeter at the periphery of the expanding zone, via feed lines R_1. If the voltmeter has a very high input impedance, there is no current flowing through the voltage measurement circuit, and the voltage it measures is the voltage between both sides of the active area, as there is no voltage drop across R_1. However, multimeters usually do have a finite input impedance (e.g. 10 MΩ), and when the resistance of the active area is high, a non-negligible portion of the measurement current will be sunk into the multimeter. This is not a problem per

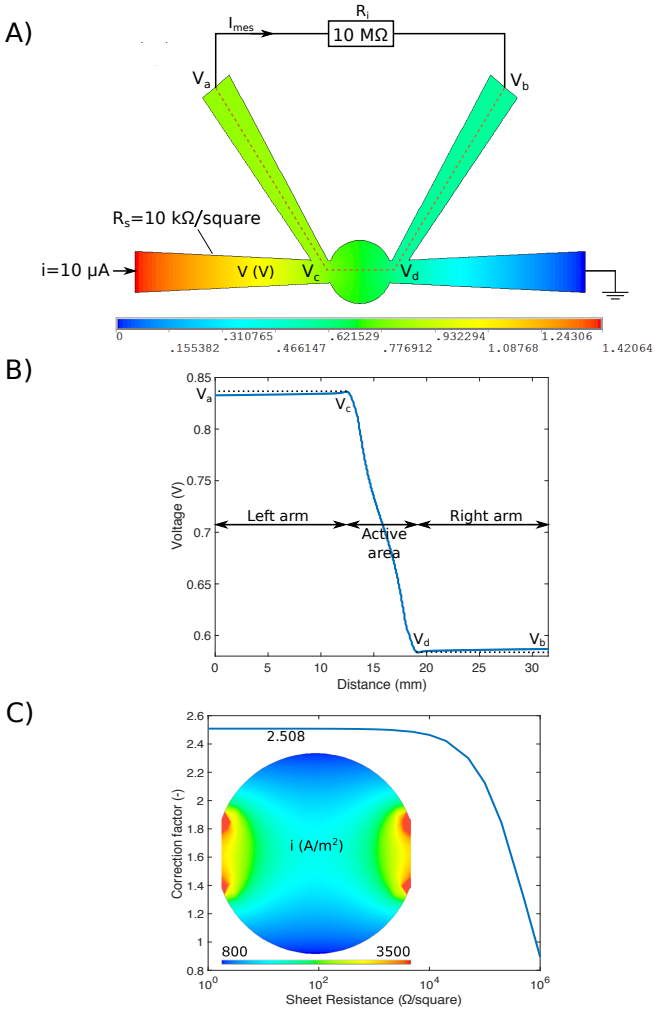

FIG. 5. Finite element analysis of the resistance measurement. A) Electrical potential (V) in the structure for an electrode with sheet resistance of 10 kΩ/square and for an input current of 10 µA when a voltmeter with an input impedance of 10 MΩ is connected to the voltage probing lines. B) Voltage potential along the dashed brown line of A). Because of the non-negligible resistance of the feed lines, the voltage measured by the voltmeter $(V_a - V_b)$ is smaller than the true voltage drop at the edge of the active area $(V_c - V_d)$. C) correction factor by which the value read on the voltmeter should be divided to obtain the sheet resistance of the electrode (i.e number of squares of the electrode). Inset: current density (A m^{-2}) in the active area for an input current of 10 µA.

se, as the multimeter is programmed to take this into account. The problem stems from the voltage drop across the feed lines R_1, which becomes non-negligible if the surface resistance of the electrode under test is high. The specifications from the Agilent 34410A multimeter state that the maximum lead resistance should be lower than 1 kΩ, a limit that can easily be exceeded for compliant electrodes, which are often based on carbon particles.

A finite element analysis (ANSYS Mechanical APDL 17.1, ANSYS Inc.) was performed to calculate the number of squares of the electrode (figure 5), i.e. the number by which to divide the resistance indicated by the multimeter to obtain the sheet resistance R_s. A geometry corresponding to the ground electrode layout was meshed with Plane 230 elements. A potential of 0 V is imposed at the end of the right arm, and a current of 10 µA is injected in the left arm. The voltage is then measured at the upper extremities of the voltage probing feed lines (V_a and V_b), corresponding to the voltage read by the multimeter. To take into account the current sunk into the multimeter with an input impedance of R_i =10 MΩ, the solution is iterated by adding a boundary condition in the form of a current $i_{mes} = (V_a - V_b)/R_i$ leaving the structure at V_a and re-entering at V_b, until an equilibrium is reached (figure 5 A). To illustrate the effect of the non-negligible resistance of the voltage probing arms, the potential along a path following the first voltage arm, crossing the circular zone, and following the second arm in the case of a 10 kΩ/square electrode and a 10 µA current injected by the multimeter is shown in figure 5 B. Because of the voltage drop in the probing arms, the voltage that the multimeter measures $(V_a - V_b)$ is smaller than the actual voltage drop across the circular electrode $(V_c - V_d)$. This difference becomes more important when the sheet resistance R_s increases. The simulation were repeated for R_s values between 1 Ω/square and 1 MΩ/square, and the correction factor (i.e. the value by which the absolute resistance displayed on the multimeter must be divided to obtain the sheet resistance R_s) is plotted in figure 5 C. A factor of 2.5 is obtained for electrode sheet resistances below 10 kΩ/square, which corresponds to the effective number of squares of the circular electrode. For a higher sheet resistance, the geometric factor is altered by the influence of the voltage probing arms.

C. Actuation Frequency

The cyclic actuation performed during the test (see figure 3) would ideally be done as fast as possible to shorten the total measurement time. However, there are 3 factors that limit the speed at which the actuation can be performed while being sure that the actuator has time to reach its full extension.

The first limiting factor is the slew rate of the high voltage power supply. The supply must indeed be able to raise to the full output voltage faster than the switching frequency. The 3 kV peta-pico-Voltron power supply used on the setup can switch from 0 V to 3 kV in 143 µs and can therefore generate square signals up to 1 kHz without difficulty (figure 6 A).

The second limiting factor is the speed at which the charges can be transported to the active area, which is linked to the *RC* time constant of the actuator. In a simplified lumped model of the actuator (figure 4), the transient current that charges/discharges the actuator capacitance (red dashed line on the figure) sees a resistance which is very similar to that seen by the resistance

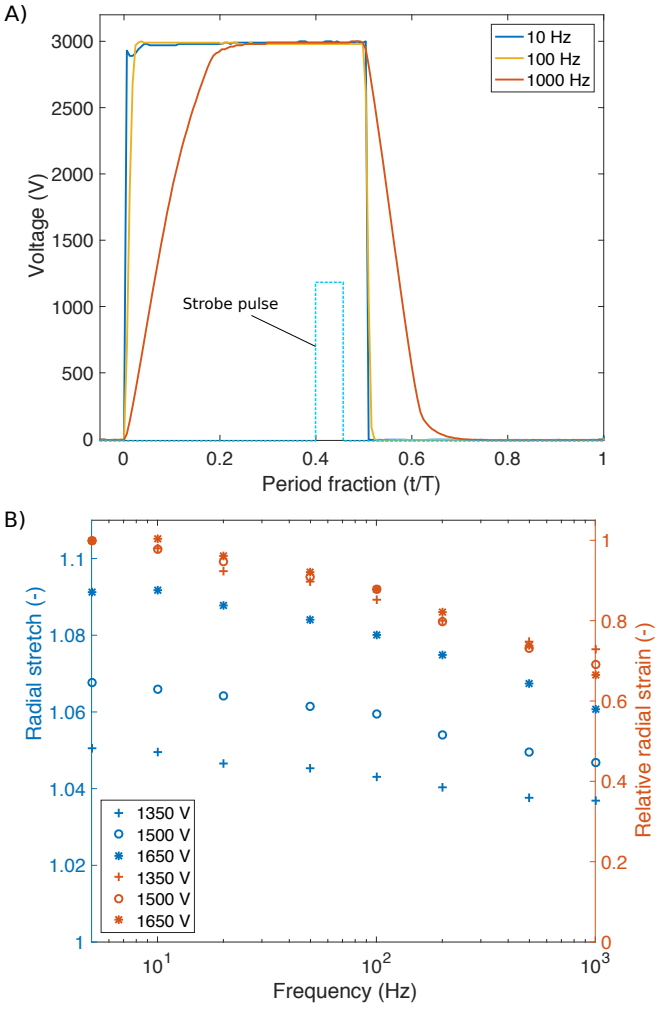

FIG. 6. A) Output voltage of the power supply as a function of time. The full voltage can be reached even at the highest tested frequency (1 kHz). B) actuator deformation (radial stretch on the left, and strain normalised at 5 Hz on the right) as a function of the driving frequency for 3 different driving voltages. The mechanical bandwidth of actuators tested on the setup (mostly the dielectric membrane) should be evaluated to select an adequate actuation frequency

measurement current flowing on the top electrode (green dashed line on the figure). Indeed, the resistance of the high voltage feed line on the bottom side of the membrane R_3 is very similar to the resistance R_2. Consequently, the resistance measured by the multimeter when it is placed in 2-wire mode (which returns a resistance value which includes the active zone, the 2 feed lines R_2, and the contact resistance) provides a good estimation of the series resistance of the actuator. The capacitance of the device can be estimated from the geometry of the test actuator. For 20 µm-thick silicone membranes, the calculated capacitance is around 20 pF, which leads to a cut-off frequency of 8 kHz for a series resistance of 100 kΩ.

The final – and usually dominating – factor limiting the response speed is the mechanical response of the actuator to the Maxwell pressure generated by the charges. Viscoelastic losses in the dielectric membrane reduce the strain when the frequency of the driving signal increases. As the data acquisition during the acquisition cycle is done in a quasi-static state, it is important to select a frequency for the cyclic actuation that is not too high, in order to ensure the same actuation stretch during the ageing phase and during the measurement phase. The mechanical bandwidth is dominated by the dielectric membrane material, although we have also previously shown that the electrodes have an impact on the response speed of DEAs[29]. We have characterised the stretch amplitude of an actuator made using a low-mechanical loss silicone (Dow Corning Sylgard 186. Refer to section IV for more information on the preparation of the samples). We have used the trigger function of the high voltage power supply to generate a voltage pulse located at 40 % of the signal period and lasting 5 % of the period (figure 6 A) to drive a LED in order to produce stroboscopic illumination to freeze the actuator in its actuated state. The experiment was performed at 3 different voltages: 1350 V leading to a steady-state stretch of 1.04, 1500 V leading to a steady-state stretch of 1.07, and 1650 V leading to a steady-state stretch of 1.095. The radial stretch for each tested voltage is represented as a function of the driving signal (square waveform) frequency on figure 6 B. The radial stretch λ is indicated in blue, and the relative radial strain normalised at the first data point is plotted in red. The relative strain shows that the frequency response is largely independent of the driving voltage amplitude. At 1 kHz, the amplitude of the periodic deformation is still about 60 % of that at 5 Hz, thanks to the low mechanical losses of the silicone elastomer used to make the actuators.

As a compromise between a rapid measurement process and the application of the desired deformation during the cyclic actuation phase, we usually run the tests at 50 Hz. This allows reaching 90 % of the desired strain during the cycles, while keeping the measurement time to reach 1 million cycles to 8 h (the 5 s stabilisation time before acquiring data during the voltage ramps and acquisition cycles (c.f. figure 3) adds to the required time to reach 1 million cycles at 50 Hz).

IV. RESULTS

To demonstrate the capabilities of the NERD test setup, we use it to evaluate the degradation and lifetime of electrodes based on a mixture of carbon black and silicone elastomer patterned by pad printing. The behaviour of the ink (initial resistance and degradation) depends on many parameters, such as the quantity of carbon black, the dispersion time and method, the thickness applied during the printing process, etc. Here, the test actuators were produced according to a protocol we published previously[30], and which represents the main method of manufacturing actuators and electrodes in our labora-

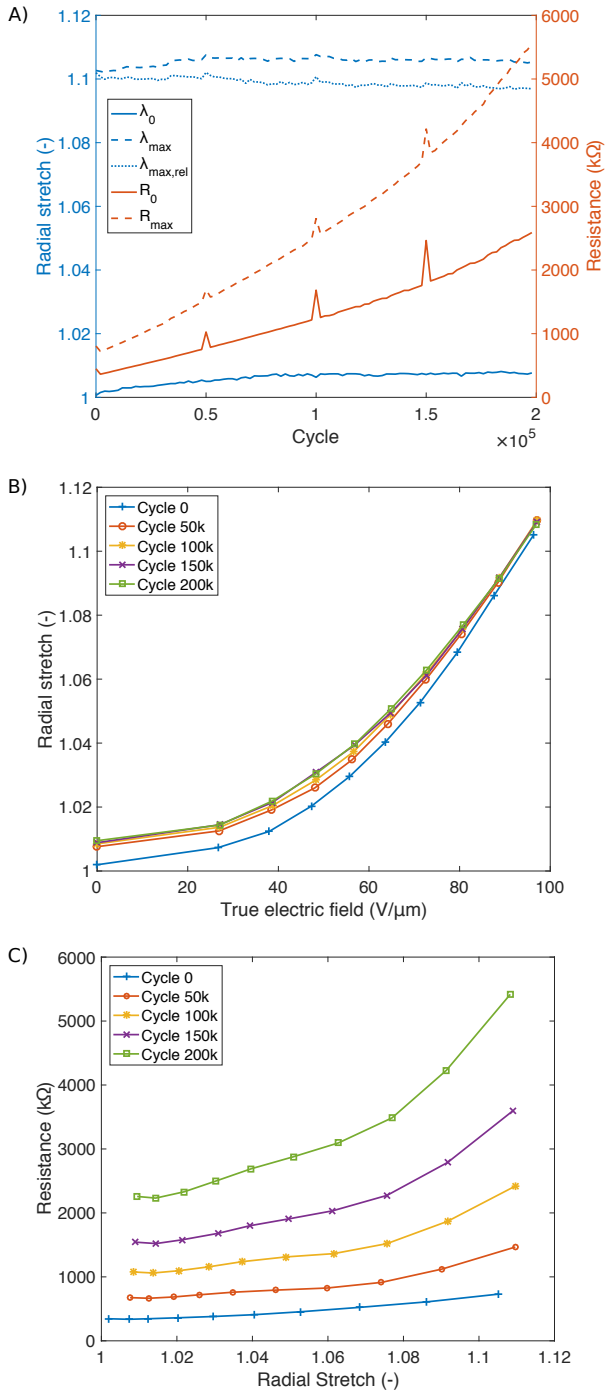

FIG. 7. 200 thousand actuation cycles at 10 % radial strain on a DEA made from a Sylgard 186 membrane with carbon composite electrodes. A) Evolution of the stretch and electrode resistance versus the number of cycles. There is a constant increase of both the unstretched and stretched resistances, while the stretch ratio remains constant. B) Radial actuation stretch as a function of applied electric field measured every 50k cycles. There is a clear increase of the stretch at rest during the first 50k cycles, but the actuation behaviour remains stable afterwards. C) Resistance versus stretch of the electrode measured every 50k cycles. Both the resistance at rest and the change of resistance when stretched are affected when the number of cycles increases.

tory. Briefly, the electrodes are made by ball-milling carbon black (Ketjenblack EC-300J from AkzoNobel) with a soft silicone elastomer and solvents. The ratio of carbon black to silicone is 1:10 by weight. The obtained ink is then patterned on the silicone membrane by pad-printing, an industrial process in which a soft silicone stamp picks up a pattern which has been doctor-bladed on a steel cliché, and applies it on the membrane.

A 28.5 µm-thick test actuator fabricated according to the protocol mentioned above is actuated for 200k cycles with a stretch of 1.10, using a driving voltage of 2250 V. Figure 7 A shows the degradation data. The resistance (red) exhibits a continuous degradation at an increasing rate. Although the resistance at rest R_0 and the resistance in the activated state R_{max} both increase, the ratio between the two, R_{max}/R_0 remains constant at a value of 2. The spikes which are seen every 50k cycles correspond to values that are measured just after the voltage ramps and reflect a resistance value which is stretch-rate dependent. This effect, which we see in the case of carbon black/silicone composite, is not present on electrodes which do not have an elastomer matrix, such as gold implanted electrodes or loose carbon powder.

The radial stretch λ, indicated in blue in the figure, can be calculated using two different reference values. The reference radius can either be the initial radius at rest, i.e. the radius at 0 V and cycle 0, $r_{0,0}$, or the reference radius can be taken as the radius of the actuator at 0 V and cycle n, $r_{0,n}$. In the first case, two different stretch ratios can be calculated: the stretch ratio at rest $\lambda_0 = r_{0,n}/r_{0,0}$, as well as the maximal stretch ratio when the test voltage V is applied: $\lambda_{max} = r_{V,n}/r_{0,0}$. In the second case, only the stretch ratio in the activated state is calculated, as the stretch ratio at rest is 1 by definition. We consequently define $\lambda_{max,rel} = r_{V,n}/r_{0,n}$. The stretch ratio calculated using the initial radius of the actuator takes the history of the sample into account. It shows that the stretch at rest λ_0 increases with the number of cycles, pinpointing a permanent deformation of the actuator which never returns to its initial size. The stretch while activated λ_{max} follows the same trend. However, the relative stretch $\lambda_{max,rel}$, which is the stretch an observer who doesn't know about the sample history would see, remains constant at 1.1.

The evolution of the stretch is best seen in the voltage ramps that are taken every 50k cycles (figure 7 B). It shows that most of the permanent deformation observed at 0 V occurs during the first 50k cycles, and that the radial stretch as a function of the electric field remains unchanged for the rest of the test. The resistance versus radial stretch and its evolution with the number of cycles (figure 7 C) show that resistance increase with both stretch and the number of cycles. Even though the degradation of the electrode during the test has no influence on the relative stretch of the device in a quasi steady-state situation, the modification of the electrical properties of the electrode (its resistance increases by a factor of about 7 over the 200k cycles) has an impact

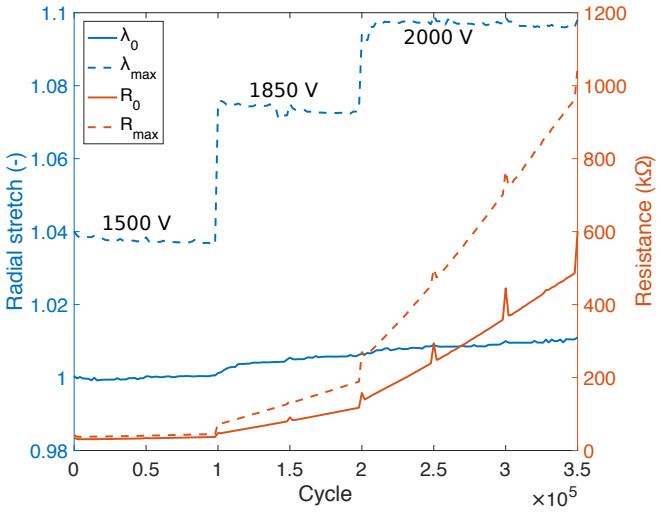

FIG. 8. Evolution of the stretch and resistance as a function of cycles when the driving voltage is changed during the test. The first 100k cycles are conducted at 1500 V for a stretch of 1.04. The following 100k cycles are conducted at 1850 V for a stretch of 1.07, and the cycles above 200k are conducted at 2000 V for a stretch of 1.095. The degradation rate of the resistance is clearly linked to the radial stretch of the actuator.

TABLE I. Resistance at 0 V (R_0) and at the test voltage V_{test} (R_{max}) at the beginning of the test and at the end of each segment.

Cycle	V_{test} (V)	λ	R_0 (kΩ)	R_{max} (kΩ)
0	-	-	38	-
1	1500	1.04	38	44
100k	1500	1.04	38	45
200k	1850	1.07	117	189
350k	2000	1.095	601	1052

on the electrical bandwidth of the actuator. In addition, the dependance of the resistance versus stretch on the number of cycles makes this electrode unsuitable to be used in a resistive self-sensing configuration, in which the absolute resistance of the device is used as a measure of the actuation stretch[31].

The degradation of the resistance of the carbon black/silicone mixture used for these tests is highly dependent on the equi-biaxial strain to which they are submitted. The resistance remains very stable for radial strains below 5 %, but increases steadily above this limit, at a rate which is stretch-dependent. Figure 8 shows the stretch and resistance evolution on 350k cycles with an actuation voltage of 1500 V for the first 100k cycles (stretch of 1.04), which is increased to 1850 V (stetch of 1.07) for the following 100k cycles, and finally to 2000 V (stretch of 1.095) for the last 150k cycles. The resistance at the beginning of the test and at the end of each segment is reported in table I. It remains stable at low actuation stretch, but increases quickly when actuated at about 10 %.

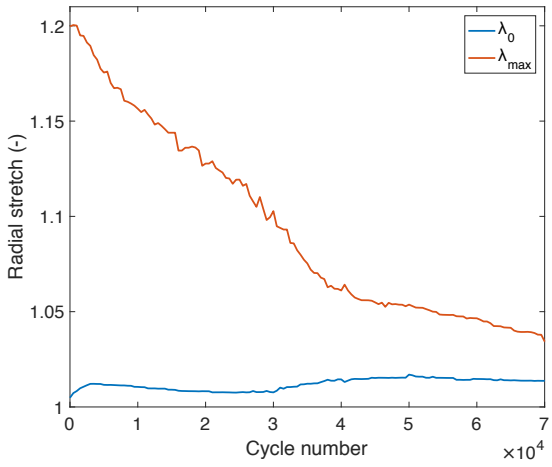

FIG. 9. Evolution of the stretch at rest (λ_0) and the maximal stretch (λ_{max}) over 70k cycles for an initial stretch of 1.2 (16.8 µm-thick Sylgard 186 membrane activated at 1700V). In addition of the residual deformation at 0 V previously observed, the maximal strain decreases by a factor 6 over 70k cycles.

The test conditions used in the preceding part of this article, for which the radial strain never exceeded 10 %, have shown important change on the resistance of the electrode, but without much influence on the strain in a steady-state situation. However, if the voltage is further increased to generate higher strains, the actuation stretch of the actuator decreases. For example, an actuator driven at a voltage that initially generates a radial actuation stretch ratio of 1.2 (in this case a 16.8 µm-thick Sylgard 186 membrane activated at 1700V) quickly sees its actuation stretch decrease (figure 9). In addition to the residual stretch in the relaxed state, the activated strain decreases by a factor of 6 over 70k cycles, a phenomenon which was not observed in the previous tests conducted for lower strains. For that particular sample, the resistance increased beyond the measurable range of the multimeter after only 2000 cycles.

The reduction in strain is due to the fact that the electrode becomes so damaged by the stretching at some locations that it is not able to charge completely (the electrode becomes essentially non-conductive). As this degradation is a local process, as opposed to the global stretch value measured by the test setup, we have used an autocorrelation image processing algorithm to measure the local strain on the pictures saved at each acquisition cycle. The algorithm is the same as the one we used to investigate the strain map induced by non-homogeneous electrodes on thin membranes[16]. The analysis has been performed on an actuator activated for an initial stretch of 22 % over 11k cycles (figure 10). As only the pictures in the activated state were available, the measurement doesn't show the absolute radial strain, but the difference with the first cycle. The bottom left corner of the active area quickly loses strain amplitude after a few thousands of cycles. At the end of the test, this part of the actuator

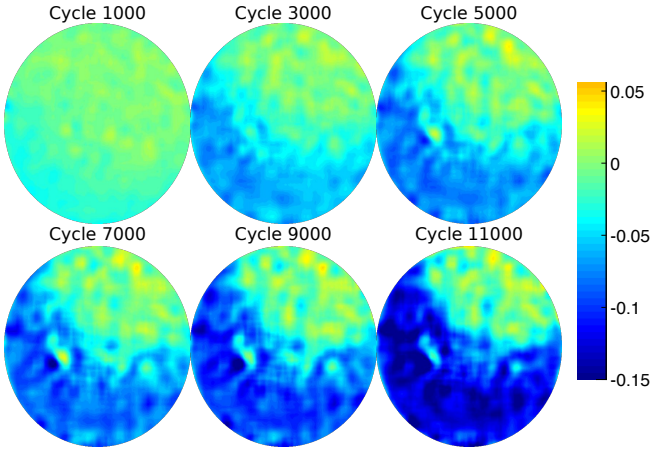

FIG. 10. Local decrease of strain compared to the actuation strain measured at the first cycle. The actuation voltage (1700 V) leads to an initial radial strain at the first cycle of 22 %. After a few thousand actuation cycles at this large strain, the electrode resistance degrades so much that part of the actuator doesn't have time to fully charge during the data acquisition phase. The linked video file shows an animated sequence of the strain decrease as a function of the number of cycles (Multimedia view).

has lost most of its actuation (−15 %), and the strain is concentrated in the upper right corner. This shows the important impact that the mechanical strain has on these carbon composite electrodes, which are quickly damaged by large equi-biaxial stretching to a point that they don't have time to charge during the 5 s voltage holding time used for the acquisition cycles.

V. CONCLUSIONS

The electrodes tested with the NERD setup are subjected to very harsh mechanical conditions. Not only is the stress equi-biaxial, pulling on the electrode material in the two orthogonal directions, but in addition, the use of a square voltage signal with a high slew rate stretches the electrodes at a high speed. However, this harsh testing is representative to what stretchable electrodes for DEAs must sustain. All DEAs are not necessarily subjected to such rough conditions (the strain can be unidirectional[32], or the actuation rate can be more gentle). However, electrodes that exhibit little to no degradation during a NERD test are sure to survive in other usage scenarii.

The testing of the carbon-black/silicone mixture patterned by pad printing that we commonly use in our laboratory showed that although this solution is fine for low strain levels (<5 %), prolonged use at higher strains causes an increase of the resistance, which reduces the electrical bandwidth (i.e. the frequency at which the actuator can be charged and discharged). If it becomes smaller than the mechanical bandwidth, then the actuator becomes electrically-limited[29].

We are currently working on improving the electrode mixture. We are therefore using the NERD setup to test different electrode compositions, working on the carbon black type, its content, its dispersion into the silicone, and its application parameters in order to optimise the mixture, and to obtain electrodes that can sustain large equi-biaxial strains without stiffening the actuator structure too much, and while keeping their resistance stable over millions of cycles. In addition, we are also investigating different electrode materials, such as conductive polymers, and different application methods, such as inkjet printing.

Because the NERD setup uses electromechanical actuation to generate the cyclic equi-biaxial strain, the strain range that can be generated is limited by the failure modes of the silicone dielectric elastomer actuators used for testing, mainly breakdown strength and electromechanical instability (EMI), effectively limiting the stretch range to below 1.25. This is suitable to evaluate the degradation of DEAs. Indeed, even if very high strains (higher than 100 % in area) were demonstrated on actuators based on acrylic elastomer materials[2,3], silicone actuators which are used for applications that require a long lifetime (for instance Optotune's laser speckle reducer[33], tuneable lenses[17], or biomedical applications[34]), linear stretches in the range of 1.05 to 1.15 are commonly used. However, the family of dielectric elastomer transducers (DETs) also encompasses generators and sensors. In their case, the source of strain is an external mechanical deformation which is not limited by breakdown or EMI, and can therefore be much larger than the stretch range that the NERD setup can provide. Consequently, electrodes that appear to show no degradation after being tested with the NERD setup should be further evaluated by different test methods if they are intended to be used in applications that require a large stretch, such as wave energy converters for example[35–37].

The novel electrode resistance degradation test setup represents a convenient way to rapidly evaluate different compliant electrodes for DEAs subjected to equi-biaxial strain by assessing their degradation when cyclically stretched and their mechanical impact on the dielectric membrane. Industrial applications of dielectric elastomer actuators require electrodes that can sustain a large number of cycles without degradation. The degradation of the electrodes and their resistance increase with the number of cycles when cyclically activated is often overlooked for lab demonstrators, which are usually tested over a limited number of cycles. However, stable electrodes are a key element for the large-scale use of DEAs in industrial applications.

ACKNOWLEDGMENTS

This work was partially supported by the Swiss National Science Foundation Grant No. 200020-165993.

[1] R. E. Pelrine, R. D. Kornbluh, and J. P. Joseph, Sensors and Actuators, A: Physical **64**, 77 (1998).
[2] R. Pelrine, R. Kornbluh, Q. Pei, and J. Joseph, Science **287**, 836 (2000).
[3] C. Keplinger, T. Li, R. Baumgartner, Z. Suo, and S. Bauer, Soft Matter **8**, 285 (2012).
[4] S. Koh, T. Li, J. Zhou, X. Zhao, W. Hong, J. Zhu, and Z. Suo, Journal of Polymer Science, Part B: Polymer Physics **49**, 504 (2011).
[5] I. A. Anderson, T. A. Gisby, T. G. McKay, B. M. O'Brien, and E. P. Calius, Journal of Applied Physics **112**, 041101 (2012).
[6] S. Rosset and H. R. Shea, Applied Physics Reviews **3**, 031105 (2016).
[7] T. G. McKay, S. Rosset, I. A. Anderson, and H. Shea, Smart Materials and Structures **24**, 015014 (2015).
[8] S. Rosset and H. Shea, Applied Physics A: Materials Science & Processing **110**, 281 (2013).
[9] M. Zhang, I. Denes, Y. Xue, and M. R. Buchmeiser, Macromolecular Chemistry and Physics **217**, 1729 (2016).
[10] A. Iannarelli and M. G. Niasar, in *Proceedings of SPIE - The International Society for Optical Engineering*, Vol. 10163, edited by Y. Bar-Cohen (SPIE, 2017) p. 1016326.
[11] M. Hodgins, A. York, and S. Seelecke, Journal of Intelligent Material Systems and Structures , 1045389X1668544 (2017).
[12] M. Hill, G. Rizzello, and S. Seelecke, in *Proceedings of SPIE - The International Society for Optical Engineering*, Vol. 10163 (International Society for Optics and Photonics, 2017) p. 101630X.
[13] H. Stoyanov, P. Brochu, X. Niu, C. Lai, S. Yun, and Q. Pei, RSC Advances **3**, 2272 (2013).
[14] W. Yuan, L. Hu, Z. Yu, T. Lam, J. Biggs, S. Ha, D. Xi, B. Chen, M. Senesky, G. Gruner, and Q. Pei, Advanced Materials **20**, 621 (2008).
[15] B. Chen, J. J. Lu, C. H. Yang, J. H. Yang, J. Zhou, Y. M. Chen, and Z. Suo, ACS Applied Materials & Interfaces **6**, 7840 (2014).
[16] A. Poulin, S. Rosset, and H. R. Shea, Applied Physics Letters **107**, 244104 (2015).
[17] L. Maffli, S. Rosset, M. Ghilardi, F. Carpi, and H. Shea, Advanced Functional Materials **25**, 1656 (2015).
[18] M. Giousouf and G. Kovacs, Smart Materials and Structures **22**, 104010 (2013).
[19] T. Töpper, F. Weiss, B. Osmani, C. Bippes, V. Leung, and B. Müller, Sensors and Actuators A: Physical **233**, 32 (2015).
[20] F. Carpi, I. Anderson, S. Bauer, G. Frediani, G. Gallone, M. Gei, C. Graaf, C. Jean-Mistral, W. Kaal, G. Kofod, M. Kollosche, R. Kornbluh, B. Lassen, M. Matysek, S. Michel, S. Nowak, B. O'Brien, Q. Pei, R. Pelrine, B. Rechenbach, S. Rosset, and H. Shea, Smart Materials and Structures **24**, 105025 (2015).
[21] S. Rosset, M. Niklaus, P. Dubois, and H. Shea, Advanced Functional Materials **19**, 470 (2009).
[22] S. Schlatter, S. Rosset, and H. Shea, in *Proceedings of SPIE - The International Society for Optical Engineering*, Vol. 10163, edited by Y. Bar-Cohen (SPIE, 2017) p. 1016311.
[23] S. Rosset, L. Maffli, S. Houis, and H. Shea, in *Proceedings of SPIE - The International Society for Optical Engineering*, Vol. 9056 (2014) p. 90560M.
[24] L. J. Van der Pauw, Philips Technical Review **20**, 220 (1958).
[25] L. J. van der Pauw, Philips Research Reports **13**, 1 (1958).
[26] J. Huang, T. Li, C. Chiang Foo, J. Zhu, D. R. Clarke, and Z. Suo, Applied Physics Letters **100**, 041911 (2012).
[27] S. Rosset, S. Schlatter, and H. Shea, "Project peta-pico-voltron," `http://petapicovoltron.com`.
[28] S. Rosset, O. A. Araromi, and H. R. Shea, Extreme Mechanics Letters **3**, 72 (2015).
[29] S. Rosset, P. Gebbers, B. M. O'Brien, and H. R. Shea, in *Proceedings of SPIE - The International Society for Optical Engineering*, Vol. 8340 (2012) pp. 834004–834004–12.
[30] S. Rosset, O. A. Araromi, S. Schlatter, and H. R. Shea, Journal of Visualized Experiments **108**, e53423 (2016).
[31] B. O'Brien, J. Thode, I. Anderson, E. Calius, E. Haemmerle, and S. Xie, in *Proceedings of SPIE - The International Society for Optical Engineering*, Vol. 6524 (SPIE, 2007) pp. 652415–11.
[32] S. Akbari, S. Rosset, and H. R. Shea, Applied Physics Letters **102**, 071906 (2013).
[33] C. Graetzel, M. Suter, and M. Aschwanden, in *Proceedings of SPIE - The International Society for Optical Engineering*, Vol. 9430 (2015) p. 943004.
[34] A. Poulin, C. S. Demir, S. Rosset, T. Petrova, and H. R. Shea, Lab on a Chip **16**, 3788 (2016).
[35] R. Vertechy, G. P. P. Rosati, and M. Fontana, Journal of Vibration and Acoustics **137**, 011004 (2015).
[36] P. Jean, A. Wattez, G. Ardoise, C. Melis, R. V. Kessel, A. Fourmon, E. Barrabino, J. Heemskerk, and J. P. Queau, in *Proceedings of SPIE - The International Society for Optical Engineering*, Vol. 8340 (2012) p. 83400C.
[37] R. D. Kornbluh, R. Pelrine, H. Prahlad, A. Wong-Foy, B. McCoy, S. Kim, J. Eckerle, and T. Low, in *Proceedings of SPIE - The International Society for Optical Engineering*, Vol. 7976 (2011) p. 797605.